



# Performance, Kinetics, and Equilibrium in Textile Dye Remediation by Agricultural Waste Biomass as A Low Cost Adsorbent

## KEYWORDS

Adsorbent, Zero point charge, Adsorption kinetics

V.Sivakumar

M. Asaithambi

P.Sivakumar

Department of Chemistry, Sri Vasavi College, Erode, TN, India -638316

Department of Chemistry, Erode Arts and Science College, Erode, India-638009

Department of Chemistry, Arignar Anna Arts College, Namakkal, TN, India-637002

**ABSTRACT** Highly active carbons X1 and X2 were prepared from the seeds of *Xanthium strumarium* L using Phosphoric acid and KOH as chemical activating agents respectively. The adsorption ability of the prepared adsorbents was analysed using Congo Red (CR) dye. The SEM images show that the adsorbent has well developed porosity with more adsorption functionalities. Both the adsorbents show a decreasing trend of adsorption on increasing the pH due to repulsion of similar charges at higher pH. Increase in sorptive removal of CR with increase in temperature may partly attribute to chemisorptions as well as endothermic nature of adsorption. Out of six isotherm models tested the Langmuir, Freundlich and Harkins-Jura isotherms are more appropriate to demonstrate the adsorption with a high correlation coefficients. Pseudo second-order model better represents the adsorption kinetics between the carbon and CR. The adsorption rate is film diffusion controlled during the initial stages of the adsorption of CR and in the later stages the rate is controlled by intra particle diffusion.

## 1.0 Introduction

Pollution of water bodies is increasing steadily due to rapid population growth, industrial proliferations, urbanisations, increasing living standards and wide spheres of human activities. The deterioration of the aesthetic and life supporting qualities of natural water resources by mixing of coloured industrial effluents containing organic dyes and inorganic complexes. The textile industries convert about 50 million tons of fibre in to textile annually. The textile industry plays an important role in the economy of the country like India and it accounts for around one third of total export. Out of various activities in textile industry, chemical processing contributes about 70% of pollution. It is well known that cotton mills consume large volume of water for various processes such as sizing, desizing, scouring, bleaching, mercerization, dyeing, printing, finishing and ultimately washing. Waste stream generated by textile industry is essentially based on water-based effluent generated in the various activities of wet processing of textiles.

Dye wastewater is commonly characterized as high in salt and organic content and low in biodegradation potential [Alinsafi, Khemis, Pons, Leclerc, Yaacoubi, Benhammou & Nejmeddine (2005)] are treated by methods like coagulation, foam flotation, filtration, ion exchange, aerobic and anaerobic treatment, advanced oxidation processes, solvent extraction, electrolysis, microbial reduction, and activated sludge. All these process have some noteworthy disadvantages, which include insufficient removal of pollutants, high capital costs, high reagents and/or energy requirements, and generation of toxic sludge or other waste products that require further safe disposal [Amit Bhatnagar, Vitor, Vilar, Cidália, Botelho, & Rui. Boaventura (2011)]. Amongst these technologies, adsorption is considered as the most versatile process. Activated carbon has been found to be a very promising adsorbent and is commonly used for the removal of diverse types of pollutants from water and wastewater [Bansal, & Goyal (2005)].

Dyes may be classified in a number of ways including colour, chemical constitution, internal use, trade name and based on application. Direct or substantive dyes are a special class of dyes which penetrate readily cellulosic fibres due to their size and shape and also have good affinity. These dyes have long narrow and flat in molecular structure, which allows them to

readily enter the cellulose structure and interact with the cellulose to provide good fibre affinity. The mixing of these dyes also deduces the dissolved oxygen content in water streams [Sivakumar, Asaithambi, Jayakumar, & Sivakumar. (2010)].

Adsorption processes using activated carbons have been widely proposed and used for the removal of both organic and inorganic pollutants from aqueous effluents. However, commercially available activated carbons are expensive and, in recent years, a great deal of effort has been put into the proposal and usage of low-cost adsorbents prepared from naturally occurring materials and wastes for the removal of dyes from wastewaters. Agricultural wastes are the chief raw materials being studied for this purpose, for they are renewable, usually available in large amounts and potentially less expensive [Reza Ansari., Babak Seyghali., Ali Mohammad-khah., & M. Ali Zanjanchi (2012)]. The most challenging are anionic dyes because they are bright coloured, water soluble, reactive and show acidic properties. Congo red (CR) is an example of anionic di azo dye discharged in waste water from textiles, printing, dyeing, paper and plastic industries [Purkait, Maiti, DasGupta, & De S. (2007)] also it is used in bio-chemistry and histology in microscopic preparations [Vijayakumar, Dharmendirakumar, Renganathan, Sivanesan, Baskar & Kuppannagounder (2009)].

The treatment of contaminated waste water with CR is not easy, since the dye is generally present in sodium salt form giving it very good water solubility. The stability of its structure makes it difficult to biodegrade, photo degrade [Vimonses, Lei, Jin, Chow, & Saint (2009)] and persists in environment Gharbani, Tabatabaai, & Mehrzad (2008)]. Attempts are made for the removal of CR by using Chitosan [Sudipta Chatterjee, Dae S.Lee, Min W.Lee, & Seung H.Woo. (2009)], Ethylenediamine modified rice hulls [Siew-Teng ong, Eng Hooi Tay., Sie-Tiong Ha., Weng-Nam Lee., & Pei-Sin Keng. (2009)], Hydrogen Peroxide treated Tendu Waste [Nagda & Ghole (2009)], Soil [Smaranda, Gavrilescu, & Bulgariu, (2011)], Bentonite [Emrah Bulut, Mahmut Ozacar, & Ayhan Sengil (2008)], Banana pith [Namasivayam, & Kanchana (1993)], rice hull ash [Kan-Sen Chou, Jyh-Ching Tsai, & Chieh-Tsung Lo. (2001)], and cashew nut hull [Senthil Kumar Ponnusamy., & Ramalingam Subramaniam. (2013)] etc. was already reported. The ability of removal of CR dye from aqueous solution by using an activated carbon prepared from, seeds of widely avail-

able weeds *Martynia annua* L and *Xanthium Strumarium* L. an agricultural waste by-product subjected to various chemical treatments was studied and reported by the same author [Vadivel Sivakumar, Manickam Asaithambi, & Ponnusamy Sivakumar. (2012)].

In this work, we have reported the performance of Phosphoric acid and KOH modified activated carbon derived from seeds of *Xanthium strumarium* L by named as X1 and X2 as a sorbent for adsorption of Congo Red, a typical anionic dye (CR) from aqueous solutions. The adsorption capacities of X1 and X2 for CR dye removal were evaluated in batch systems. Batch experiments were performed for finding the optimized dye removal conditions and obtaining adsorption isotherms.

The influence of various operating parameters such as the effect of pH influent dye concentration, temperature also reported. The equilibrium and kinetic parameters are studied to describe the velocity and mechanism of adsorption process to determine the factor controlling the adsorption rate and to realize the possibility of using of these agricultural waste derived activated carbons as low-cost adsorbents for the removal of CR. The physical nature and surface morphology of the adsorbent had been known on the basis of their SEM images, XRD, and BET isotherm studies.

## 2.0 Materials and Methods

### 2.1 Adsorbent preparation

Seeds of *Xanthium strumarium* L collected from Erode District, Tamilnadu, India were used for the preparation of adsorbent. The waste seed were thoroughly rinsed with water to remove dust and the soluble material and was allowed to dry at room temperature. The dried natural waste was treated with Phosphoric acid and KOH. After impregnation, the excess acid/base was decanted. The treated mass was subjected to carbonization at 400 °C and powdered well. It was washed with excess of water to confiscate excess acids present. The material was sieved activated at 800 °C for a period of 10 minutes.

### 2.2 Characteristics of adsorbent

The preparation and physico-chemical characterization of X1 and X2 activated carbons was already reported in the previous paper [Vadivel Sivakumar et al (2012)]. Carbon particles with a mesh size of 350 to 125 $\mu$  were taken for the adsorption studies. The specific surface area and the pore structure of the Carbon samples were determined by using a surface area and pore size analyzer (Micrometrics, ASAP 2020 V3.00 H Instrument) on nitrogen adsorption at -195.759 °C. The specific surface area was calculated using the BET equation. The BET data, BJH Desorption Pore Distribution Report, Horvath-Kawazoe Report of X3 and BET data of X4 were listed in Table 1.

The microstructures of X1 and X2 carbons were observed by Scanning Electron Micrograph (JOEL/EO 1.1 Model: JSM 5610) and are shown in Fig. 1a and 1b.

### 2.3 Preparation of Adsorbate

Congo red was supplied by Chamundi Textiles (Silks Mills) LTD, Mysore, India. A stock solution of CR dye was prepared (1000 mg/L) by dissolving a required amount of dye powder (based on percentage purity) in deionized water. The stock solution was diluted with deionized water to obtain the desired concentration ranging from 10 to 75 mg/L. The concentration of CR in the experimental solution was determined by measuring the absorbance of CR solutions at  $\lambda_{max}$ =498nm using a UV-Vis spectrophotometer (Perkin-Elmer).

### 2.4 Adsorption Studies

The pH of the solution was measured with a Elico pH meter (model LI 120) using a combined glass electrode. Adsorption experiments were conducted as per the design developed with response surface central composite design methodol-

ogy. The experiments were carried out in 250-mL Erlenmeyer flasks with the working volume of 100 mL of reaction mixture containing fixed carbon dosage of 100 mg of respective carbon samples. The initial pH of the solution was adjusted to the desired value by adding 0.1 M NaOH or HCl. The flasks were shaken for the specified time period in 150 rpm in an orbital shaker (Rivotec). The flasks were withdrawn from the shaker after the desired time of reaction. The residual dye concentration in the reaction mixture was analyzed by centrifuging (5,000 rpm, R-24 REMI Centrifuge) the reaction mixture and then measuring the absorbance of the supernatant at the wavelength that corresponds to the maximum absorbance of the sample.

The effect of initial pH for 50mg/L dye concentration was studied in the pH range from 2 to 10 with a fixed carbon dosage agitated for 2 hours at room temperature. The effect of temperature on adsorption was studied at four different temperatures from 35 to 60°C for 75mg/L dye solution with a fixed carbon dosage (100mg/100mL). The amount of dye adsorbed per unit mass of the adsorbent q mg/g and adsorption efficiency were calculated as follows:

$$\text{Efficiency (\%)} = \frac{(C_0 - C)}{C_0} \times 100 \text{ ----- (1)}$$

Where,  $C_0$  = initial dye concentration (mg/L),  $C$  = residual dye concentration (mg/L),

## 3.0 Results and discussion

### 3.1 Adsorbent Characteristics

#### 3.1.1 Scanning Electron Micrographs (SEM)

The scanning electron microscopic (SEM) micrographs of X1 and X2 are shown in Fig. 1a and 1b respectively. The SEM of X1 (Fig. 1a) indicates a heterogeneous, porous morphology. Based on the BET analysis carried out for X1 and X2, the specific surface area of X1 was found to be more (279.6774 m<sup>2</sup>/g) compared with X2 (4.5547 m<sup>2</sup>/g). So, it might be concluded that dye uptake by X2 is not governed by its surface area; instead the surface chemistry of the X2 due to the presence of various functional groups determines its sorption properties. Where as carbon X1 having larger surface area the dye uptake property governed by presence of long pores inside in it evident by its SEM images.

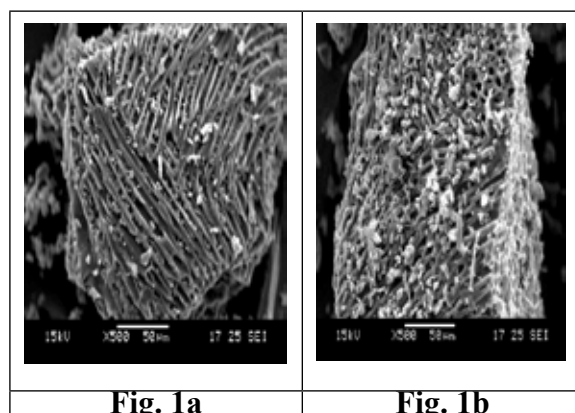
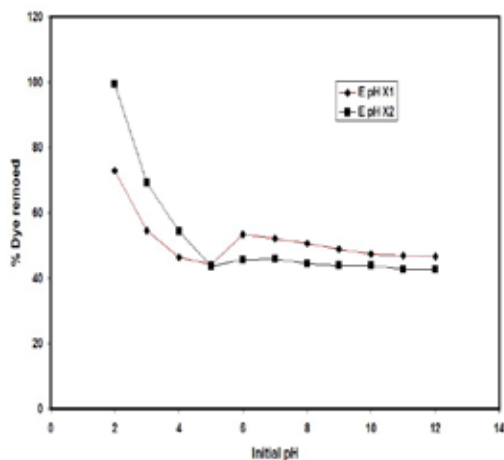


Fig. 1a & 1b – SEM images of X1 and X2

### 3.2 Effect of Solution pH value on dye adsorption

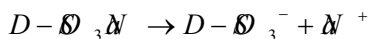
The pH affects the structural stability of CR which leads to change in its colour intensity [14]. Aqueous solution of CR turns blue in colour at lower pH and it turns red colour in higher pH values. At lower pH values it exists as dipolar molecule ( $H_3N^+ -R-X-3$ ). The experiments carried out at different pH from 2 to 12 shows that there is a change in the per cent removal of dyes over the entire pH range which is shown in the Fig. 2. In carbon X1 the percentage of CR removal decreases from 73 at pH 2 to 44 at pH 5. When pH reaches 6 the removal percent increases from 44 to 54. This large

increase may be because of the zero point charge of the carbon X1. The reported pHzpc of carbon X1 is 6.2 and X2 is 7.8 [Vadivel Sivakumar et al]. At the zero point charge, the carbon surface doesn't have any charge and the adsorption of CR begins without electrostatic interaction between dye molecule and surface groups on the carbon. Both the carbons show considerable increase in adsorption percent at their respective  $pH_{zpc}$ . Initially there is a drastic decrease in dye removal was observed in carbon X2 from 99.5% to 44% while increasing the solution pH 2 to 6. After this pH, a slight increase in CR removal was observed near its pHzpc. The dye removal further decreases and it reaches 46.5% for carbon X1 and 42.5% for X2 at solution pH reaches 12.



**Figure 2 – Effect of pH for the adsorption of CR onto X1 and X2**

From electro kinetic studies of carbon surfaces, the nature and the concentration of the surface charge can be modified by changing the pH of the solution. The surface of the carbon attained positive charge below its zero point charge and becomes negative charge above its zero point charge to a certain range of pH. In the aqueous phase, the dye is first dissolved and the sulfonate groups of the dye (D-SO<sub>3</sub>Na) are dissociated and converted to anionic dye ions at natural solution pH of 6.8 [Emrah Bulut, Mahmut Ozacar, & Ayhan Sengil (2008)]. At pH below the isoelectric point, a dye exists predominantly in the molecular form, while above the isoelectric point it exists with a higher proportion in its dissociated form. The isoelectric point of CR is 3, thus CR would be exists in the form of negatively charged sodium diphenyl diazo-bis- -naphthylamine-4-sulfonate ions at pH range 5.0 to 10.0 [Emrah Bulut et al, Zhang, Moghaddam, O'Hara, & Doherty (2011)].



At lower pH excessive protonation leads the carbon surface more positive in nature. Lower pH is favoured for the electrostatic interaction between carbon and CR. However, the presence of -N=N- and -NH<sub>2</sub> groups in CR and they will be protonized in a much lower pH solution. The protonizing of these groups is not favourable for this interaction. The negatively charged dye molecules attracts by them through strong electrostatic force of attraction. The amount of positive nature decreases while increase the solution pH, the dye removal also decreases. But at  $pH_{zpc}$  the carbon surface is neutral and the intrusion of dye molecules in to the pores of the adsorbent prevails without electronic forces. The surface area of the carbon X1 is considerably higher compared with carbon X2. The electrical neutrality of carbon X1 increases the adsorption process more than 10% in to its pores than carbon X2 at  $pH_{zpc}$ . Since it has lesser surface area, only 3%

enhanced removal is observed near at neutral pH.

### 3.3 Effect of Temperature

The effect of temperature for the adsorption of CR (75mg/L) on X1 and X2 were carried out at five different temperatures from 30 to 60°C. The percentage of colour removal slowly decreases in X1 from 63 to 60 up to 40°C. Raise in 10°C doesn't enhance the dye adsorption. Whereas in X2 even 5°C raise in temperature increase the dye up taking ability up to 20%. It implies high temperature favours the CR removal in X2. This may be because of increase in mobility of the large dye ion.

The enhancement of adsorption capacity of the adsorbent at high temperatures may be also attributed to the enlargement of pore size and activation of the adsorbent surface. Since it posses very low surface area at normal temperature, increase in temperature increasing the number of molecules may acquire sufficient energy to undergo an interaction with available active sites on the carbon surface. Therefore increase in sorptive removal of CR with increase in temperature may partly attribute to chemisorptions. The increase in the adsorption capacity upon increasing the temperature indicates that each adsorption was an endothermic process. In X1 adsorption through physical forces prevails, temperatures have no effect on dye removal. Further raise in temperature from 40°C to 60°C it is observed that the dye adsorption is decreases in both the carbons.

### 3.4 Equilibrium isotherms for CR adsorption on activated carbon

The mechanism of adsorption can be studied by various adsorption isotherms. Adsorption isotherm usually describes the equilibrium concentration of adsorbate in the bulk of the solution and amount adsorbed at the surface. Analysis of isotherm data is fundamentally important to predict the adsorption capacity of the adsorbent for designing an adsorption system. The data obtained were analysed according to the Langmuir, Freundlich, Temkin, Dubinin-Radushkevich (D-R), Harkins-Jura and Halsey isotherm models. The linear, non-linear equations, plots of these isotherm models are shown in Table 2.

#### 3.4.1 Langmuir Isotherm

The correlation of the experimental adsorption data with a number of adsorption models was undertaken to gain an understanding of the adsorption behaviour and the heterogeneity of the adsorbent surface. The Langmuir Isotherm assumes monolayer coverage of adsorbate on finite number of uniformly energetic adsorption sites within the adsorbent surface, with no lateral interaction and steric hindrance between the adsorbed molecules. Once an adsorbate molecule occupies a site, no further adsorption can take place at that site. Thus, an equilibrium value can be reached and the saturated monolayer curve can be expressed by this equation. The linear form of Langmuir isotherm is presented in Table. 2. Where,  $C_e$  is the equilibrium concentration of CR (mg/L) in the solution,  $q_e$  is the amount of CR adsorbed per unit mass of adsorbent (mg/g),  $Q_0$  and  $b_1$  are constants related to adsorption capacity (mg/g) and energy of adsorption (L/mg). Plot of  $C_e/q_e$  against  $C_e$  gave straight line with positive slope ( $1/Q_0$ ) and intercept with  $b_1$  (Fig.3a and 3b) indicating the adsorption of CR on X1 and X2 follows the Langmuir isotherm. The Langmuir isotherm was found to be linear over the entire concentration range with good linear correlation coefficients ( $0.9081 < R^2 < 0.964$  for carbon X1 and  $0.9355 < R^2 < 0.9913$  for carbon X2) fits the experimental data very well. It may be due to the homogeneous distribution of active sites onto the surface.

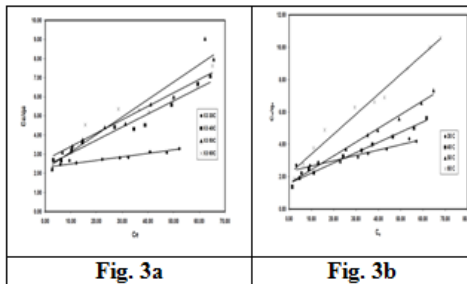


Fig. 3a & 3b – Langmuir Plot for the adsorption of CR onto X1 and X2

Langmuir adsorption capacity  $Q_0$  slightly increases from 12.315 at 30°C to 14.641 at 40°C for X1. Increasing of temperature may increase the pore width and accommodates few more dye molecules per unit weight of the adsorbent. The swelling of adsorption sites decreases the maximum amount of adsorbate to form a complete monolayer on X2 is evidenced by continuous decrease of its  $Q_0$  values from 30.121 at 30°C to 8.130 at 60°C. In both the carbons the affinity of CR molecules on active sites on the surface of the adsorbent is not too high. Decreasing of intermolecular attractive forces to the raise of the distance is confirmed by its calculated  $b$  values.

The essential characteristics of Langmuir isotherm can be expressed in terms of a dimensionless equilibrium parameter  $R_L$  defined by Weber and Chakravorti [Ho, & McKay (1999)] is.

$$R_L = \frac{1}{(1 + bL C_0)} \quad \text{----- (2)}$$

Where,  $C_0$  is the initial concentration of CR in mg/L,  $R_L$  value indicated the type of adsorption isotherm to be either unfavourable ( $R_L > 1$ ), favourable ( $R_L < 1$ ), linear ( $R_L = 1$ ) or irreversible ( $R_L = 0$ ).

The adsorption of CR on to X1 and X2 is favourable at the four temperatures evident from its calculated  $R_L$  values (0.4576 <  $R_L$  < 0.5584 for X1 and 0.3930 <  $R_L$  < 0.6179 for X2). The calculated values of Langmuir constants  $b_L$ ,  $Q_0$ , correlation coefficient, dimensionless equilibrium parameter  $R_L$  were listed in Table 3.

**3.4.2 Freundlich isotherm model**

This model can be applied to non-ideal and reversible multilayer adsorption systems on heterogeneous surfaces; it has not restricted the monolayer formation. The linearized form of Freundlich equation is given in Table 2. Where  $K_f$  is the measure of adsorption capacity (L/g),  $n$  is the adsorption intensity and are calculated from intercept and slope respectively are listed in Table 3 from the linear plot of  $\log q_e$  versus  $\log C_e$  (Fig. 4a and 4b). The slope ranges between 0 and 1 is a measure of adsorption intensity or surface heterogeneity, becoming more heterogeneous as its value closer to zero. The value of  $1/n$  is below unity implies chemisorption's process where above one is an indicative of cooperative adsorption [Haghsereht & Lu (1998)].

The calculated  $n$  values show that at normal temperature the dye adsorption may influenced by physical forces and when raising the temperature only chemical forces predominates in both the carbons. The slope ( $1/n$ ) values are decreased and closer to zero when increasing the temperature indicates the surface becomes more heterogeneous and the possibility of swelling of the adsorption sites at higher temperature has confirmed. It concludes at 30°C the CR removal includes cooperative adsorption and the surfaces are homogeneous nature and the increasing of temperature the surfaces become more heterogeneous and chemisorption process prevails. Both the carbon samples indicate that the adsorption of CR

is favourable. The experimental data's are excellently fitted with this equation with high correlation coefficient values for X1 (0. 0.9388 <  $R^2$  < 0.9952) and X2 (0.9556 <  $R^2$  < 0.9675).

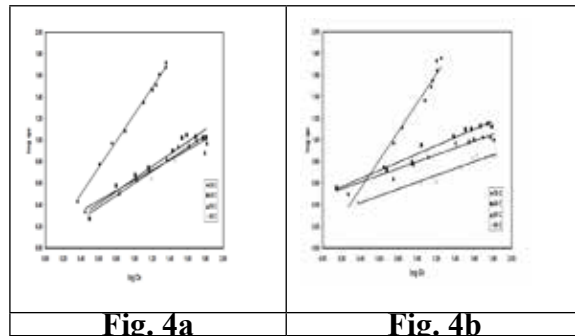


Fig. 4a & 4b – Freundlich Plot for the adsorption of CR onto X1 and X2

**3.4.3 Temkin model**

The linear and non linear forms of Temkin equation is given in Table 2. Where  $A$  is the equilibrium binding constant corresponding to the maximum binding energy (L/mg),  $B$  is Temkin isotherm constant (J/mol),  $B$  is a dimensionless constant related to heat of adsorption (function of temperature),  $R$  is the gas constant (8.314J/mole). The values of the Temkin constants  $A$  and  $B$  calculated from the intercept and slope respectively and correlation coefficients are listed in Table 3 from the linear plot of  $\ln C_e$  versus  $q_e$  (Figure not shown). This model contains a factor that explicitly taking in to account of adsorbate- adsorbent interactions [Templin & Pyzhev (1940)].

The maximum binding energy ( $A$ ) is noted in X1(0.680) at 40°C implies the interaction of CR molecules with the adsorption sites is more when we raise the temperature and it stabilises (0.4879 at 50°C and 0.4668 at 60°C) further raising the temperature. The value of  $B$  is high at 30°C and it is further decreased when increase the temperature. This indicates that at lower temperature more molecules are gets adsorbed on X1, hence the heat of adsorption is more (7.5137). The value of  $B$  is also stabilized at higher temperature (3.2926 at 50°C and 3.0041 at 60°C). In X2, the value of  $A$  increases to larger extent (0.3599 to 1.5556) when the temperature changes from 30°C to 40°C respectively. This implies when a system is influenced by thermal properties it shows maximum binding energy. Whereas at lower temperature the heat of adsorption ( $B$ ) is more (5.6593 at 30°C) and it decreases drastically at higher temperatures (1.5029 at 60°C).

**3.4.4 Dubinin-Radushkevich model**

The linear form of D-R isotherm is shown in Table 2. Where  $q_e$  is the amount of CR adsorbed on to per unit dosage of Carbon (mol/g),  $q_m$  is the theoretical monolayer adsorption capacity (mol/g),  $\beta$  is the constant related to adsorption energy (mol<sup>2</sup> /J<sup>2</sup>).  $\epsilon$  is Polanyi potential which is described as

$$\epsilon = R \cdot T \cdot \ln \left( 1 + \frac{1}{C_e} \right) \quad \text{----- (3)}$$

Where,  $R$  is the gas constant (8.314J/mole) and  $T$  is the absolute temperature in K. This model is usually applied to distinguish the physical and chemical adsorption of adsorbate molecules with its mean free energy  $E$  (KJ/mole) per molecule of adsorbate can be calculated by the following relationship

$$E = \frac{1}{\sqrt{2\beta}} \quad \text{----- (4)}$$

The value of  $E$  ranges from 1 to 8 KJ/mole for physical sorption and from 8 to 16 KJ/mole for chemical sorption [Sharply

(1983)]. Unique features of the D-R isotherm model lies on the fact that it is temperature dependent, which when the adsorption data at different temperatures are plotted as a function of natural logarithm of amount adsorbed versus the square of potential energy yields the values of  $q_m$  and  $\beta$  from the intercept and slope of the plot (Figure not shown) and are listed in Table 3. As seen from the values, DR isotherm does not fit with experimental data. It shows very low correlation coefficients for both the carbon indicates that the adsorption of CR on to X1 and X2 does not follow Dubinin-Radushkevich model.

**3.4.5 Halsey isotherm model**

The Halsey isotherm model is used for heteroporous solids. It is suitable for multilayer adsorption. The equation is given in Table 2. Where  $K$  is the Halsey isotherm constant and  $n$  is the exponent. Plot of  $\ln C_e$  vs  $\ln q_e$  gives a negative  $n$  values (Figure not shown) and the value of  $K$  is calculated from the intercept are listed in Table 3. The existence of long pores favours the multi-layer adsorption in X1 and the data obtained are fitted with minimum correlation coefficient values  $0.6548 < R^2 < 0.8052$  implies the presence of physical forces in the adsorption process is ruled out. The existence of surface heterogeneity is not ruled out in the adsorption of CR on to X2 because the obtained data are fairly fitted with the equation  $0.8745 < R^2 < 0.9367$ .

**3.4.6 Harkins–Jura isotherm model**

The linear and non linear form of Harkins-Jura isotherm equation is given in Table 2. Where  $C_e$  is the equilibrium concentration of CR in solution (mg/L),  $q_e$  is the amount of CR adsorbed onto the adsorbent (mg/g) and  $A$   $B$  are isotherm constants. The Harkins-Jura adsorption isotherm accounts to multilayer adsorption and can be explained with the existence of a heterogeneous pore distribution.  $1/q_e^2$  was plotted vs  $\log C_e$  (figure not shown) and the isotherm constants, correlation coefficient values are listed in Table 3. This method can be employed when different types of pores are involved in an adsorbent. Both the carbon samples have slits and spherical pores on its surface. It is confirmed by its SEM images and data obtained from XRD studies. The experimental data obtained are fitted to this equation with high correlation coefficients ( $0.9952 > R^2 > 0.9388$  for X1 and  $0.9675 > R^2 > 0.9556$  for X2). This implies the existence of surface heterogeneity at all temperatures in the adsorbent helps the trapping of dye molecules inside the pores. The surface of the adsorbent containing the pores which are not in uniform size and they are distributed unevenly.

By comparing the correlation coefficients  $R^2$  calculated to Langmuir, Freundlich, Temkin, DR, Halsey, Harkins-Jura isotherms can be deduced that the experimental equilibrium sorption data are well described by the Langmuir, Freundlich, Temkin, Harkins-Jura models, when the correlation coefficients were high at 30, 40 50 and 60°C. The Freundlich isotherm assumes that there is a continuously varying energy of sorption as the most actively energetic sites are occupied first and the surface is continually occupied until the lowest energy sites are filled at the end of the process. All the four models fitted with the experimental data with high correlation coefficient values.

**3.5 Adsorption Kinetics**

Adsorption kinetics show large dependence on the physical and chemical characteristics of the adsorbent material, and adsorbate species present in bulk and which also influence the sorption mechanism. In the present work in order to examine the controlling mechanism of sorption processes such as mass transfer and chemical reaction pseudo first-order kinetic, pseudo second- order, intraparticle diffusion and elovich kinetic models are used.

**3.5.1 Pseudo-first order Kinetic Model**

The equation for first- order kinetics can be written as

$$\log(q_e - q_t) = \log q_e - \frac{k_1}{2.303} t \quad \text{----- (5)}$$

Where,  $q_e$  and  $q_t$  are the amounts of CR adsorbed at equilibrium and time  $t$  (min) respectively,  $k_1$  is the first-order rate constant ( $\text{min}^{-1}$ ). Linear plot of  $\log (q_e - q_t)$  versus  $t$  was made and values of  $k_1$  and  $q_e$  were obtained from the slope and intercept (figure not shown) as given in table 4.

The results shows that adsorption of CR onto X1 doesn't follow the first order kinetics. At the given temperature, the first-order rate constant ( $k_1$ ) increases with the increase in initial dye concentration. This may be because at higher initial dye concentration, the number of available binding sites, at the X1 surface, per adsorbate molecule, increases. The obtained  $R^2$  and  $q_e$  values for carbon X2 shows the dye removal processes does not follow first order kinetics. The adsorption data fitted poorly with pseudo-first order kinetic model for both carbon samples and the calculated  $q_e$  values are does not agree with the experimental  $q_e$  values at all concentrations. Hence the adsorption does not follow first order rate expression for both the carbons. The CR removal process does not depend on either the concentration of adsorbent system or adsorbate availability in the bulk.

**3.5.2 Pseudo-second order Kinetic Model**

Pseudo second-order model rate equation is represented as

$$\frac{t}{q_t} = \frac{1}{k_2 q_e^2} + \frac{1}{q_e} t$$

Where  $h = k_2 q_e^2$  ----- (6)

Where,  $h$  represents the initial adsorption rate ( $\text{mg/g min}$ ) and  $k_2$  is the second order rate constant ( $\text{g/mg min}$ ). The values of  $k_2$  and  $q_e$  were calculated from the intercept and slope of the  $t/q_t$  versus  $t$  plots as shown in fig 5a and 5b and the results are given in table 4. It can be seen from table 4 that there is an agreement between experimental and calculated  $q_e$  values with high correlation coefficient values for both the carbons. Hence the Pseudo second-order model better represents the adsorption kinetics between the carbon and CR. The adsorption process depends on the concentration of both the species such as adsorbent and adsorbate. The rate of adsorption processes depends on concentration of carbon and CR molecules in the bulk.

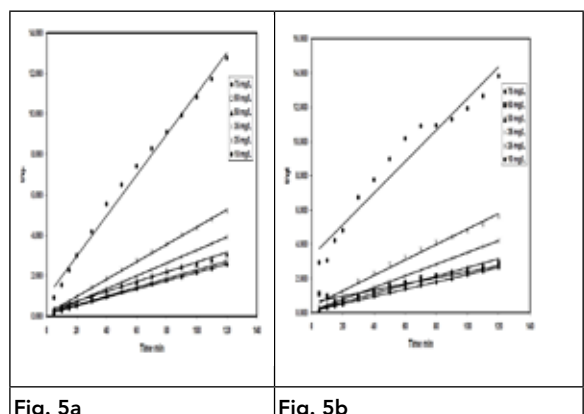


**Fig. 5a & 5b – Pseudo-second order plot for the adsorption of CR onto X1 and X2**

**3.5.3 Elovich model**

The adsorption data may also be analysed by using the Elovich equation which has the form

$$\frac{dq}{dt} = \alpha e^{-\beta q} \quad \text{----- (7)}$$

Where,  $k_1$  is the initial adsorption rate constant (mg/g min) and  $k_2$  is related to the extent of surface coverage and activation energy for chemisorptions (g/mg). If we assume that  $k_2 \gg 1$  and the integration of the rate equation with the same boundary conditions as the pseudo first-order and second-order equations becomes the Elovich equation

$$q_t = \frac{1}{\beta} \ln(\beta) + \frac{1}{\beta} h t \text{ ----- (8)}$$

The values of  $k_1$ ,  $k_2$  calculated from intercept and slop obtained by plotting  $\ln t$  vs.  $qt$  are listed in Table 4 along with  $R^2$  values (figure not shown).

Some investigators have used  $k_1$  and  $k_2$  parameters derived from elovich equation to estimate reaction rates. For example, it has been suggested that an increase in  $k_1$  value and/or decrease in  $k_2$  value would increase the rate of the adsorption process. The slope of the plots obtained by using equation 8 changes with the concentration of adsorptive and with the dye-to-carbon ratio. The obtained  $R^2$  values for both the carbons for all the concentrations are considerably high ( $0.9018 < R^2 < 0.9845$  for X1 and  $0.8619 < R^2 < 0.9454$  for X2). This suggests that elovich model best describes this adsorption system.

**3.5.4 Weber- Morris model**

The Weber- Morris or Intra particle diffusion model describes the adsorption of dye solutes from solution by porous carbon consists three consecutive steps [Weber (1972)]. The first step is the transport of the dye from the bulk solution to the outer surface of the carbon by molecular diffusion. This is called external or film diffusion. The concentration gradient in the liquid film around the carbon surface is the driving force in film diffusion. The second step, called internal diffusion, which involves transport of the dye from the carbon surface into interior sites by diffusion within the pore filled liquid and migration along the solid surface of the pore. These two steps act in parallel, the more rapid one will control the overall rate of transport. The third and final step is adsorption of the dye on the active sites on the interior surface of the pores. The overall rate of the adsorption process will be controlled by the slowest step among the three steps.

Since adsorption step is very rapid one, the rate controlling step is either film diffusion or internal diffusion. The nature of the rate determining step in batch systems can be determined from the properties of solute and adsorbent. Rates of adsorption are usually measured by determining the change in concentration of the dye in contact with the carbon as a function of time.

The intra- particle diffusion equation is given as

$$q_t = K_p t^{1/2} \text{ ----- (7)}$$

**Table 1 - Textural characteristics of activated carbon**

Carbon	S <sub>BET</sub> (m <sup>2</sup> /g)	Total pore Volume cm <sup>3</sup> /g	Molecular cross-sectional area (nm <sup>2</sup> )	Radius Range Å	Maximum Pore Volume (cm <sup>3</sup> /g)	Median Pore Width Å	Q <sub>m</sub> cm <sup>3</sup> /g STP
X1	279.677	0.9939: 0.13224	0.1620	8.500 to 1500.00	0.132238	7.651	64.2464
X2	4.555	0.9971: 0.0292	0.1620	-	-	-	1.0463

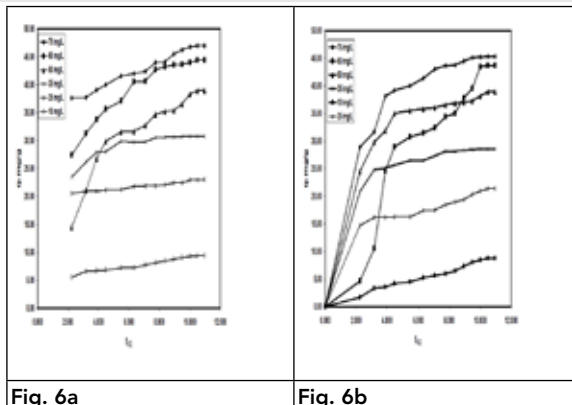


**Fig. 6a & 6b – Intra particle diffusion plot for the adsorption of CR onto X1 and X2**

Where,  $K_p$  is the intra-particle diffusion rate constant (mg/g min<sup>1/2</sup>) and  $C$  is calculated from the intercept while plotting the graph between amounts of dye adsorbed  $qt$  and  $t^{1/2}$  (Fig. 6a and 6b). From the plots adsorption of CR by X1 is film diffusion controlled at concentrations less than 35mg/L and a direct linear relationship exists between the initial CR concentration and adsorption rate. If the concentration of CR exceeds 35 mg/L, the reaction was shown to be intra particle diffusion controlled. In carbon X2 the CR concentration exceeds 25 m/L the process is controlled by intra particle diffusion. The obtained  $R^2$  and  $K_p$  values are shown in Table 4. It is recognized that the adsorption rate is film diffusion controlled during the initial stages of the adsorption of CR process in batch systems and the carbon becomes loaded with more adsorbate molecules the reaction rate becomes controlled by intra particle diffusion.

**Conclusion**

An activated carbon with good adsorption characteristics were successfully prepared from the seeds of *Xanthium strumarium L* using Phosphoric acid and KOH as chemical activating agents. The specific surface area of X1 was found to be more (279.6774 m<sup>2</sup>/g) compared with X2 (4.5547m<sup>2</sup>/g). The prepared adsorbents were tested for its adsorption ability toward the textile dyes. The direct dye Congo red shows good affinity toward both the adsorbents. Lower pH is very effective for the removal of CR as the adsorption CR on X1 and X2 decreases with increase of pH. Out of Six isotherm models, the Langmuir, Freundlich and Harkins-Jura model fits the data with high correlation coefficients. The kinetics is CR adsorption onto X1 and X2 follows pseudo-second order kinetics. The initial stages of adsorption follows film diffusion mechanism and the later stages were controlled by intra particle diffusion. An activated carbon prepared from the seeds of *Xanthium strumarium L* is a promising adsorbent for the removal of dye molecules from their respective wastewater.

Table 2 - Lists of adsorption isotherms models

Isotherm model	Nonlinear form equation	Linear form equation	Plot
Langmuir	$q_e = \frac{Q_0 b C_e}{1 + b C_e}$	$\frac{C_e}{q_e} = \frac{1}{Q_0 b_L} + \frac{C_e}{Q_0}$	$\frac{C_e}{q_e}$ Vs $C_e$
Freundlich	$q_e = K_f C_e^{1/n}$	$\log q_e = \log K_f + \frac{1}{n} \log C_e$	$\log q_e$ Vs $\log C_e$
Temkin	$q_e = \left(\frac{RT}{b}\right) \ln(A C_e)$	$q_e = \left(\frac{RT}{b}\right) \ln A + \left(\frac{RT}{b}\right) \ln C_e$	$\ln C_e$ Vs $q_e$
Dubinin-Raduskevich	$q_e = q_m e^{-K \varepsilon^2}$	$\ln q_e = \ln q_m - \beta \varepsilon^2$	$\varepsilon^2$ Vs $\ln q_e$
Harkins-Jura	$m = n \ln C_e + \frac{1}{q_e^2}$	$\frac{1}{q_e^2} = \left(\frac{B}{A}\right) - \left(\frac{1}{A}\right) \log C_e$	$1/q_e^2$ Vs $\log C_e$
Halsey	$\ln q_e = \left[\left(\frac{1}{n}\right) \ln K\right] + \left(\frac{1}{n}\right) \ln \frac{1}{C_e}$	$\log q_e = \left(\frac{1}{n}\right) \log K + \left(\frac{1}{n}\right) \log \frac{1}{C_e}$	$1/C_e$ Vs $\ln q_e$
BET	$q_e = \frac{q_s C_{BET} C_e}{(C_s - C_e)[1 + (C_{BET} - 1)\left(\frac{C_e}{C_s}\right)]}$	$\frac{C_e}{q_e(C_s - C_e)} = \frac{1}{q_s C_{BET}} + \frac{(C_{BET} - 1) C_e}{q_s C_{BET} C_s}$	$\frac{C_e}{q_e(C_s - C_e)}$ Vs $\frac{C_e}{C_s}$

Table 3 - Results of Various adsorption isotherm models

	30°C		40°C		50°C		60°C	
	X1	X2	X1	X2	X1	X2	X1	X2
<b>Langmuir</b>								
$Q_0$ (mg/g)	12.3153	30.1205	14.6413	15.7480	10.9649	11.7509	14.3062	8.1301
$b_L$ (L/mg)	0.0351	0.0143	0.0289	0.0401	0.0413	0.0585	0.0257	0.0565
$R_L$	0.4919	0.6179	0.5342	0.4637	0.4576	0.4040	0.5584	0.3930
$R^2$	0.9081	0.9355	0.964	0.9865	0.9392	0.9913	0.9284	0.9794
<b>Freundlich</b>								
$K_f$ (mg/g)	1.0069	1.0500	1.1671	3.0875	1.4174	3.0409	1.1179	1.9575
$n$	0.8094	0.7563	1.7437	2.6337	2.1088	3.1656	1.8113	3.1636
$1/n$	1.24	1.32	0.573	0.379	0.474	0.316	0.552	0.316
$R^2$	0.9952	0.963	0.9515	0.9675	0.9388	0.9556	0.9648	0.9559
<b>Temkin</b>								
$A$ (L/g)	0.3140	0.3599	0.680	1.5556	0.4879	2.4723	0.4668	1.7498
$B$	7.5137	5.6593	2.4989	3.0281	3.2926	2.1329	3.0041	1.5029
$R^2$	0.9314	0.9725	0.900	0.9481	0.9445	0.9376	0.9261	0.9161
<b>D-R</b>								
$\beta$	-1.9782	-0.0006	0.0036	0.0044	-0.0023	-0.0011	-0.0031	-0.0005
$X_m$	257.632	1.0250	8.7615	12.8115	7.2510	5.8223	7.6895	8.5901
$E$	0.5027	-28.90	-11.78	-10.66	14.75	-21.32	12.71	-31.65
$R^2$	0.6529	0.5856	0.7881	0.8172	0.661	0.5612	0.688	0.5338
<b>Halsey</b>								
$n$	-1.2413	-1.3731	-1.7436	-2.6337	-2.1088	-3.1656	-1.8112	-3.1636
$K$	0.9931	0.9341	0.7637	0.0514	0.4792	0.0296	0.8173	0.1195
$R^2$	0.7352	0.8887	0.6548	0.8745	0.8052	0.9155	0.7517	0.9367
<b>Harkins-Jura</b>								
$A$	8.5837	22.3214	6.3052	24.8756	8.1633	24.3309	6.4558	12.6582
$B$	10.1150	1.6987	1.6450	1.7214	1.7143	1.8491	1.6856	1.9468
$R^2$	0.9952	0.963	0.9515	0.9675	0.9388	0.9556	0.9648	0.9559

## REFERENCE

- Ahmad, R., & Kumar, R. (2010). Adsorptive removal of Congo red dye from aqueous solution using bael shell carbon, *Appl. Surf. Sci.* 257, 1628-1633 | Alinsafi, Khemis, M., Pons, M.N., Leclerc, J.P., Yaacoubi, A., Benhammou, A., & Nejmeddine, A. (2005). Electro-coagulation of reactive textile dyes and textile wastewater, *Chem Eng Process*, 44, 461-470. | Amit Bhatnagar, Vitor, J.P., Vilar, Cidália, M.S., Botelho., & Rui. Boaventura, A.R. (2011). A review of the use of red mud as adsorbent for the removal of toxic pollutants from water and wastewater, *Environmental Technology*, 32 (3), 231-249. | Bansal, R.C., & Goyal, M. (2005). Activated Carbon Adsorption, CRC Press, Boca Raton, FL. | Emrah Bulut., Mahmut Ozacar., & Ayhan Sengil I. (2008). Equilibrium and kinetic data and process design for adsorption of Congo red on to bentonite, *J. Haz. Mat.* 154, 613-622. | Gharbani, P., Tabatabaie, & S.M., Mehrizad, A. (2008). Removal of Congo red from textile waste water by ozonation, *Int. J. Environ. Sci. Tech.* 5, 495-500. | Haghseresh, F., & Lu, G. (1998). Adsorption characteristics of phenolic compounds onto coal-reject derived adsorbents, *Energy Fuels*. 12, 1100-1107. | Ho, Y.S., & McKay, G. (1999). Pseudo-Second-Order Model for Sorption Processes", *Process Biochemistry*, 34, 451-465. | Kan-Sen Chou., Jyh-Ching Tsai., & Chieh-Tsung Lo. (2001). The sorption of Congo red and vacuum pump oil by rice hull ash, *Bioresource Technol.* 78, 217-219 | Nagda., G. K., & Ghole, V. S. (2009). Biosorption of Congo red by Hydrogen Peroxide treated Tendu Waste, *Iran. J. Environ. Health. Sci. Eng.* 6, 195-200. | Namasivayam., & Kanchana, N. (1993). Removal of Congo red from aqueous solution by waste banana pith, *Pertanika J. Sci. & Technol.* 1, 33-42. | Purkait, M.K., Maiti, A., DasGupta, S., & De S. (2007). Removal of Congo red using activated carbon and its regeneration, *J. Haz. Mat.* 145(1-2), 287-295. | Reza Ansari., Babak Seyghali., Ali Mohammad-khah., & M. Ali Zanjanchi (2012). Highly Efficient Adsorption of Anionic Dyes from Aqueous Solutions Using Sawdust Modified by Cationic Surfactant of Cetyltrimethylammonium Bromide, *J. Surfact Deterg.* 15, 557-565. | Senthil Kumar Ponnusamy., & Ramalingam Subramaniam. (2013). Process optimization studies of Congo red dye adsorption onto cashew nut shell using response surface methodology, *International Journal of Industrial Chemistry*, 4, 17 | Sharply, A. N. (1983) Effect of soil properties on the kinetics of phosphorous desorption, *Soil Sci. Soc. Am. J.* 47, 462 | Siew-Teng ong., Eng Hooi Tay., Sie-Tiong Ha., Weng-Nam Lee., & Pei-Sin Keng. (2009). Equilibrium and continuous flow studies on the sorption of Congo red using ethylenediamine modified rice hulls, *Int.J.Phy. Sci.* 4(11) 638-690. | Sivakumar, V., Asaithambi, M., Jayakumar, N., & Sivakumar, P. (2010). Assessment of the Contamination from the Tanneries & Dyeing Industries on to Kalingarayan Canal of Tamilnadu *Int.J. ChemTech Res* 2, 774-779 | Smaranda., Gavrilescu., & Bulgariu, D. (2011) Studies on sorption of Congo red from aqueous solution on to soil, *Int. J. Environ. Res.*, 5:177-188. | Sudipta Chatterjee., Dae S.Lee., Min W.Lee., & Seung H.Woo. (2009) Enhanced adsorption of Congo red from aqueous solutions by chitosan hydrogel beads impregnated with cetyl trimethyl ammonium bromide. *Bioresource Technology*, 100, 2803-2809 | Tempkin, M.I., & Pyzhev, V. (1940). Kinetics of ammonia synthesis on promoted iron catalyst, *Acta Phys. Chim. USSR.* 12, 327-356. | Vadivel Sivakumar., Manickam Asaithambi., & Ponnusamy Sivakumar. (2012) Physico-chemical and adsorption studies of activated carbon from Agricultural wastes, *Adv. App. Sci. Res.* 3 (1), 219-226 | Vijayakumar, G., Dharmendirakumar, M., Renganathan, S., Sivanesan, S., Baskar, G., & Kuppanagounder, P. E. (2009). Removal of Congo red from aqueous solutions by perlite, *Clean-Soil Air Water*, 37, 355-364. | Vimonses, V., Lei, S., Jin, B., Chow, C. W. K., & Saint, C. (2009). Adsorption of Congo red by three Australian kaolins. *Appl. Clay. Sci.* 43, 465-472. | Weber W. J. (1972) *Physicochemical processes for water quality control*, Wiley- inter sciences, New York. | Zhang, Z., Moghaddam, L., O'Hara, I.M., & Doherty, W.O.S. (2011). Congo red adsorption by ball-milled sugarcane bagasse, *Chem. Eng. J.* 178, 122- 128. |